American Journal of Computational Mathematics, **2011, 1, 39-54**
doi:10.4236/ajcm.2011.12005 Published Online June 2011 (http://www.scirp.org/journal/ajcm)

Scientific Research

Characteristic Analysis of Exponential Compact Higher Order Schemes for Convection-Diffusion Equations

Sanyasiraju V. S. S. Yedida, Nachiketa Mishra
Department of Mathematics, Indian Institute of Technology Madras, Chennai, India
E-mail: *sryedida@iitm.ac.in, mishra.nachiketa@gmail.com*
Received February 19, 2011; *revised March* 23, 2011; *accepted April* 5, 2011

Abstract

This paper looks at the development of a class of Exponential Compact Higher Order (ECHO) schemes and attempts to comprehend their behaviour by introducing different combinations of discrete source function and its derivatives. The characteristic analysis is performed for one-dimensional schemes to understand the efficiency of the scheme and a similar analysis has been introduced for higher dimensional schemes. Finally, the developed schemes are used to solve several example problems and compared the error norms and rates of convergence.

Keywords: Exponential Scheme, Compact Higher Order Scheme, Characteristics, Resolving Efficiency, Finite Difference

1. Introduction

Many interesting engineering problems involve the physical processes and transport phenomena that include fluid flow, heat and mass transfer, can be modelled by a general Convection-Diffusion Equation (CDE). This equation describes the convection and diffusion characteristics of various physical quantities, such as momentum, energy, concentration, etc. This paper deals with the numerical solution of convection-diffusion equation of the form

$$-au_{xx} - bu_{yy} + cu_x + du_y = f(x, y) \qquad (1)$$

on $\Omega \subset R^2$, with boundary conditions

$$u(x, y) = g(x, y) \quad \text{on} \quad \partial\Omega, \qquad (2)$$

where $a, b > 0$ are constant diffusion, c, d are constant convection coefficients and f, g are sufficiently smooth functions with respect to x and y. If $0 < a$, $b << 1$ are very small when compared with c and d, then (1) becomes a convection dominated equation for which [1-4] are some of the exponential schemes known from the literature. For higher dimensional problems, though the schemes [2-4] are all fourth order accurate, scheme presented in [4] seems to be giving better results over the other two. The purpose of this work is to understand the good features of the scheme given in [4] and based on these features include some additional conditions in the development of ECHO schemes. Since the development of these schemes is already been discussed in [4], instead of repeating the same in this work, we focus on understanding the merits of the scheme. Section two presents a new class of ECHO schemes for 1D CDE, their classification and numerical verification. Echo schemes for 2D CDE are formulated and compared in the Section three and conclusions are drawn in the last section.

2. 1D Convection-Diffusion Equations

The one dimensional equivalent of (1), by fixing $b = d = 0$, is given by

$$-au_{xx} + cu_x = f(x), \quad 0 < x < 1, \qquad (3)$$

with boundary conditions $u(0) = g_1$, $u(1) = g_2$, where g_1, g_2 are some constants.

2.1. ECHO Schemes

A general strategy to develop ECHO schemes is by starting with the difference equation

$$-\alpha D_h^2 u_i + cD_h u_i = F_i \qquad (4)$$

where $D_h u_i = (u_{i+1} - u_{i-1})/2h$ and $D_h^2 u_i = (u_{i+1} - 2u_i + u_{i-1})/h^2$ over a uniformly distributed nodal points with step length h and F_i is a linear combination of the source term f_i and its derivatives at a chosen number

of stencil (mesh) points with equal number of arbitrary constants (refer [2-4] for three such different choices). α is taken to be $\frac{ch}{2}\coth\left(\frac{ch}{2a}\right)$ when the convection coefficient $c \neq 0$ so that the difference Equation (4) is exact for $e^{\left(\frac{cx}{a}\right)}$ otherwise it is equal to a. If F_i is taken as f_i then (4) is a second order compact exponential scheme which was discussed in [5]. In the development of the ECHO scheme, the arbitrary constants in F_i are obtained by making the difference Equation (4) is exact for x, x^2, $x^3, \cdots$ In this work four different stencils are used for F_i and the corresponding constants have been computed by forcing the difference scheme (4) to be at least fourth order accurate. The four chosen stencils and their constants are given by (refer [3,4] for the complete derivation of the computation of the coefficients).

2.1.1. Stencil-1

Consider the discrete source function

$$F_i = c_1 f_{i-1} + c_2 f_i + c_3 f_{i+1} + c_4 (f_x)_i \qquad (5)$$

where f_i, $(f_x)_i$ are the source function and it's derivative, respectively, at the nodal point i. The Equation (4) is already exact for $\left\{1,\ e^{\left(\frac{cx}{a}\right)}\right\}$ and enforcing the exactness also for $\left\{x,\ x^2,\ x^3,\ x^4\right\}$ gives four simultaneous equations in terms of its coefficients. Solving them for c_i, $i = 1,\ 2,\ 3\ \&\ 4$ gives

$$c_1 = \frac{1}{6} - 3\beta^3 + \beta^2 - 0.5\beta + 3\beta^2\gamma - \beta\gamma + 0.25\gamma,$$

$$c_2 = \frac{2}{3} - 2\beta^2 + 2\beta\gamma,$$

$$c_3 = \frac{1}{6} + 3\beta^3 + \beta^2 + 0.5\beta - 3\beta^2\gamma - \beta\gamma - 0.25\gamma,$$

$$c_4 = h\left(-6\beta^3 - 0.5\gamma + 6\beta^2\gamma\right),\quad \beta = \frac{a}{ch},\quad \gamma = \frac{\alpha}{ch}$$

for $c \neq 0$

and $c_1 = \frac{1}{12},\ c_2 = \frac{5}{6},\ c_3 = \frac{1}{12},\ c_4 = 0$ when $c = 0$.

Similarly for the other stencils, system of equations are obtained and solved to get the corresponding co-efficients.

2.1.2. Stencil-2

$$F_i = c_1 f_i + c_2 (f_x)_{i-1} + c_3 (f_x)_i + c_4 (f_x)_{i+1} \qquad (6)$$

when $c \neq 0$ the coefficients are

$$c_1 = 1,$$

$$c_2 = h\left(\frac{1}{6}\beta + \beta^3 - 0.5\beta^2 - \frac{1}{12} - \frac{1}{12}\gamma - \beta^2\gamma + 0.5\beta\gamma\right),$$

$$c_3 = h\left(\frac{2}{3}\beta - 2\beta^3 - \frac{5}{6}\gamma + 2\beta^2\gamma\right),$$

$$c_4 = h\left(\frac{1}{6}\beta + \beta^3 + 0.5\beta^2 + \frac{1}{12} - \frac{1}{12}\gamma - \beta^2\gamma - 0.5\beta\gamma\right)$$

and $c_1 = 1,\ c_2 = \frac{-h}{24},\ c_3 = 0,\ c_4 = \frac{h}{24}$ for $c = 0$.

2.1.3. Stencil-3

$$F_i = c_1 f_i + c_2 (f_x)_i + c_3 (f_{xx})_i + c_4 (f_{xxx})_i, \qquad (7)$$

when $c \neq 0$ the coefficients are

$$c_1 = 1,\ c_2 = h(\beta - \gamma),\ c_3 = h^2\left(\frac{1}{6} + \beta^2 - \beta\gamma\right),$$

$$c_4 = h^3\left(\beta^3 + \frac{1}{6}\beta - \beta^2\gamma - \frac{1}{12}\gamma\right),$$

and $c_1 = 1,\ c_2 = 0,\ c_3 = \frac{h^2}{12},\ c_4 = 0$ for $c = 0$.

2.1.4. Stencil-4

$$F_i = c_1 f_{i-1} + c_2 f_i + c_3 f_{i+1} + c_4 (f_x)_i + c_5 (f_{xx})_i \qquad (8)$$

when $c \neq 0$ the coefficients are

$$c_1 = 12\beta^4 - 3\beta^3(1+4\gamma) + \beta^2(2+3\gamma) - \beta(0.5+\gamma) + (0.1+0.25\gamma),$$

$$c_2 = -24\beta^4 + 24\beta^3\gamma - 4\beta^2 + 2\beta\gamma + 0.8,$$

$$c_3 = 12\beta^4 + 3\beta^3(1-4\gamma) + \beta^2(2-3\gamma) + \beta(0.5-\gamma) + (0.1-0.25\gamma),$$

$$c_4 = -h(6\beta^3 - 6\beta^2\gamma + 0.5\gamma),$$

$$c_5 = -h^2\left(12\beta^4 - 12\beta^3\gamma + \beta^2 - \frac{1}{15}\right),$$

and $c_1 = \frac{1}{30},\ c_2 = \frac{14}{15},\ c_3 = \frac{1}{30},\ c_4 = 0,\ c_5 = \frac{h^2}{20}$

for $c = 0$.

Schemes with stencils 1, 2 and 3 contain four parameters and are fourth order accurate, whereas the scheme with stencil 4 contains five parameters and is sixth order accurate. Here after, we refer the difference scheme (4) with stencils 1 to 4 as schemes $S_1^{[1D]}$ to $S_4^{[1D]}$, respectively for all the future references. Exponential schemes of [2,3] are also fourth order accurate with three arbitrary parameters and the scheme given in [4] uses six parameters to generate a sixth order scheme for the chosen one-dimensional convection-

diffusion equation. The discrete source terms of these schemes [2-4] are given by.

Stencil used in [2]:

$$F_i = c_1 f_{i-1} + c_2 f_i + c_3 f_{i+1} \tag{9}$$

$c_1 = \frac{1}{6} + \beta^2 - 0.5\beta - \beta\gamma + 0.5\gamma$, $c_2 = \frac{2}{3} - 2\beta^2 + 2\beta\gamma$,

$c_3 = \frac{1}{6} + \beta^2 + 0.5\beta - \beta\gamma - 0.5\gamma$ when $c \neq 0$,

$c_1 = \frac{1}{12}$, $c_2 = \frac{5}{6}$, $c_3 = \frac{1}{12}$ when $c = 0$.

Stencil used in [3]:

$$F_i = c_1 f_i + c_2 (f_x)_i + c_3 (f_{xx})_i \tag{10}$$

$$c_1 = 1,\ c_2 = h(\beta - \gamma),\ c_3 = h^2\left(\beta^2 + \frac{1}{6} - \beta\gamma\right)$$

when $c \neq 0$,

$$c_1 = 1,\ c_2 = 0,\ c_3 = \frac{h^2}{12} \text{ when } c = 0.$$

Stencil used in [4]:

$$\begin{aligned} F_i = {} & c_1 f_{i-1} + c_2 f_i + c_3 f_{i+1} \\ & + c_4 (f_x)_{i-1} + c_5 (f_x)_i + c_6 (f_x)_{i+1} \end{aligned} \tag{11}$$

when $c \neq 0$ the coefficients are

$$\begin{aligned} c_1 = {} & 90\beta^5 - (12 + 90\gamma)\beta^4 + (7.5 + 12\gamma)\beta^3 \\ & - (0.5 + \gamma)\beta + \frac{7}{30} + 0.375\gamma \end{aligned},$$

$$c_2 = 24\beta^4 + \frac{8}{15} - 24\beta^3\gamma + 2\beta\gamma,$$

$$\begin{aligned} c_3 = {} & 90\beta^5 - (12 + 90\gamma)\beta^4 + (7.5 + 12\gamma)\beta^3 \\ & - (0.5 + \gamma)\beta + \frac{7}{30} + 0.375\gamma \end{aligned},$$

$$c_4 = h\begin{pmatrix} 30\beta^5 - 6\beta^4(1 + 5\gamma) + (3.5 + 6\gamma)\beta^3 \\ -(0.5 + \gamma)\beta^2 + \left(\frac{1}{30} + 5\gamma\right) \end{pmatrix},$$

$$c_5 = h(120\beta^5 - 120\beta^4\gamma + 8\beta^3 + 2\beta^2\gamma - \gamma),$$

$$c_6 = h\begin{pmatrix} 30\beta^5 + 6\beta^4(1 - 5\gamma) + (3.5 - 6\gamma)\beta^3 \\ +(0.5 - \gamma)\beta^2 - \left(\frac{1}{30} - 5\gamma\right) \end{pmatrix},$$

and $c_1 = \frac{2}{15}$, $c_2 = \frac{11}{15}$, $c_3 = \frac{2}{15}$, $c_4 = \frac{h}{40}$, $c_5 = 0$, $c_6 = \frac{-h}{40}$ for $c = 0$.

Name the scheme (4) with stencils used in [2-4] as schemes $S_5^{[1D]}$, $S_6^{[1D]}$ and $S_7^{[1D]}$, respectively. That is, a total of seven ECHO schemes have been introduced until now and out of which five of them are fourth order accurate and the other two are sixth order accurate. Among the fourth order schemes, three of them, developed in this work, have four free parameters and the other two, taken from the literature [2] and [3], have three parameters. Among the sixth order schemes, one scheme developed in this work has five free parameters and the other taken from the literature $S_7^{[1D]}$ has six parameters. That is, the seven schemes can be classified into n^{th} order schemes with n number of parameters and the other contain less than n number of parameters. The aim of the rest of the work is to demonstrate, using wave number analysis and numerical experimentation, the n^{th} order ECHO schemes with n parameters are more accurate than the other class of schemes.

2.2. Comparison of the Characteristic Curves

Using the wave number analysis, resolution of any numerical scheme can be measured with which one can understand the closeness of the characteristic of a difference equation to that of the differential equation [6]. Since the stability of any numerical scheme depends on the magnitude of the peclet number, defined by $p = \frac{ch}{\varepsilon}$, in this work, the characteristics are compared with respect to peclet numbers. The characteristic of the governing Equation (1), obtained by substituting e^{Iwx} in the place of the dependent variable u, is given by:

$$\lambda^{[1D]} = \frac{c}{h}\left(\frac{\varphi^2}{p} + I\varphi\right) \tag{12}$$

where $\varphi = wh$, w is the wave number, $I = \sqrt{-1}$. Similarly, the characteristics of the difference schemes are obtained by substituting $e^{Ii\varphi}$ at u_i to get (refer [4,6] for more details).

Characteristic Curve for $S_1^{[1D]}$:

$$\lambda_1^{[1D]} = \frac{c}{h}\left(\frac{\gamma w'' + Iw'}{z_2 + Iz_1}\right) \tag{13}$$

where $w' = \sin\varphi$, $w'' = 2 - 2\cos\varphi$, $\gamma = \frac{1}{2}\left(\coth\frac{p}{2}\right)$,

$z_1 = \mu_4\varphi + (\mu_3 - \mu_1)\sin\varphi$, $z_2 = (\mu_3 + \mu_1)\cos\varphi$,

$$\mu_1 = \frac{1}{p^3}\left(p^3\left(0.25\gamma + \frac{1}{6}\right) - p^2(\gamma + 0.5) + p(3\gamma + 1) - 3\right),$$

$$\mu_2 = \frac{1}{p^2}\left(\frac{2}{3}p^2 + 2\gamma p - 2\right),$$

$$\mu_3 = \frac{-1}{p^3}\left(p^3\left(0.25\gamma - \frac{1}{6}\right) + p^2(3\gamma - 1) - p(\gamma - 0.5) + 3\right),$$

$$\mu_4 = \frac{-1}{p^3}(0.5\gamma p^3 - 6\gamma p - 6).$$

Characteristic Curve for $S_2^{[1D]}$:

$$\lambda_2^{[1D]} = \frac{c}{h}\left(\frac{\gamma w'' + Iw'}{z_2 + Iz_1}\right) \tag{14}$$

where

$$w' = \sin\phi, \quad w'' = 2 - 2\cos\varphi,$$
$$\gamma = \frac{1}{2}\left(\coth\frac{p}{2}\right), z_1 = \mu_3\varphi + (\mu_4 + \mu_2)\varphi\cos\varphi,$$
$$z_2 = \mu_1 - (\mu_4 - \mu_2)\varphi\sin\varphi, \quad \mu_1 = 1,$$
$$\mu_2 = \frac{-1}{p^3}\left(p^3 + p^2\left(\frac{1}{12}\gamma - \frac{1}{6}\right) - 0.5p(\gamma - 1) + (\gamma - 1)\right),$$
$$\mu_3 = \frac{1}{p^3}\left(-p^2\left(\frac{5}{6}\gamma - \frac{2}{3}\right) + 2p(\gamma - 1)\right),$$
$$\mu_4 = \frac{1}{p^3}\left(p^3 - p^2\left(\frac{1}{12}\gamma - \frac{1}{6}\right) - 0.5p(\gamma - 1) - (\gamma - 1)\right).$$

Characteristic Curve for $S_3^{[1D]}$:

$$\lambda_3^{[1D]} = \frac{c}{h}\left(\frac{\gamma w'' + Iw'}{z_2 + Iz_1}\right) \tag{15}$$

where

$$w' = \sin\varphi, \quad w'' = 2 - 2\cos\varphi, \quad \gamma = \frac{1}{2}\left(\coth\frac{p}{2}\right),$$
$$z_1 = \varphi(\mu_2 - \mu_4\varphi^2), \quad z_2 = \mu_1 - \mu_3\varphi^2, \quad \mu_1 = 1,$$
$$\mu_2 = \frac{1}{p}(1 - p\gamma), \quad \mu_3 = \frac{1}{p^2}\left(1 + \frac{1}{6}p^2 - p\gamma\right),$$
$$\mu_4 = \frac{1}{p^3}\left(1 + \frac{1}{6}p^2 - p\gamma - \frac{1}{12}p^3\gamma\right).$$

Characteristic Curve for $S_4^{[1D]}$:

$$\lambda_4^{[1D]} = \frac{c}{h}\left(\frac{\gamma w'' + Iw'}{z_2 + Iz_1}\right) \tag{16}$$

where $\theta(\lambda)$ [2]S4

$$w' = \sin\varphi, \quad w'' = 2 - 2\cos\varphi, \quad \gamma = \frac{1}{2}\left(\coth\frac{p}{2}\right),$$
$$z_1 = \mu_4\varphi + (\mu_3 - \mu_1)\sin\varphi,$$
$$z_2 = \mu_2 - \mu_5\varphi^2 + (\mu_3 + \mu_1)\cos\varphi,$$
$$\mu_1 = \frac{1}{p^4}(12 - 3p(1 + 4\gamma) + p^2(2 + 3\gamma) - p^3(0.5 + \gamma) + p^4(0.1 + 0.25\gamma)),$$

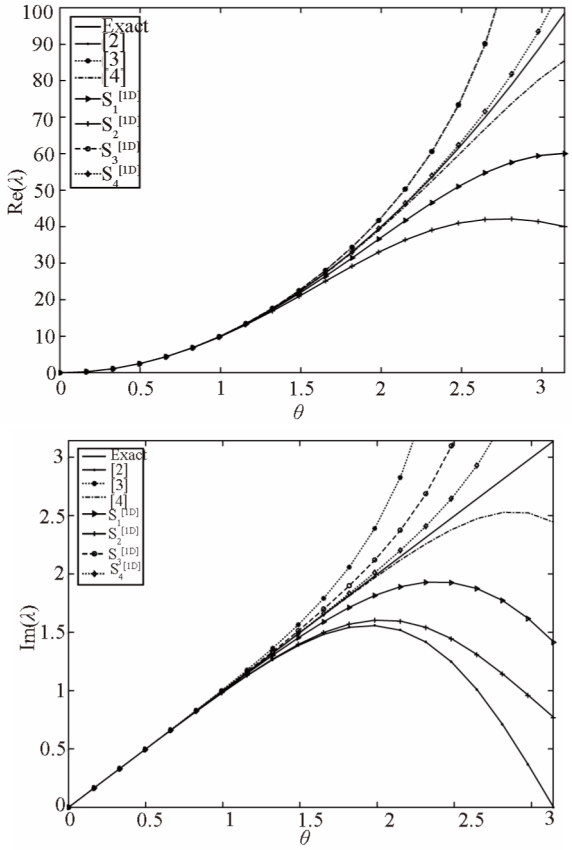

Figure 1. Comparison of real and imaginary parts of $\lambda^{[1D]}$ at $p = 0.1$.

$$\mu_2 = \frac{1}{p^4}\{-24 + 24p\gamma - 4p^2 + 2p^3\gamma + 0.8p^4\},$$
$$\mu_3 = \frac{1}{p^4}(12 + 3p(1 - 4\gamma) + p^2(2 - 3\gamma) + p^3(0.5 - \gamma) + p^4(0.1 - 0.25\gamma)),$$
$$\mu_4 = \frac{-1}{p^3}(6 - 6p\gamma + 0.5p^3\gamma),$$
$$\mu_5 = \frac{-1}{p^4}\left(12 - 12p\gamma + p^2 - \frac{1}{15}p^4\right).$$

Both real and imaginary parts of the characteristics (13-16) are compared with (12) in **Figures 1**, **2** and **3** for peclet numbers 0.1, 10 and 100, respectively. For the sake of comparison, the characteristics of the Schemes $S_5^{[1D]}$, $S_6^{[1D]}$ and $S_7^{[1D]}$, are also included in these figures. It is clear from these comparisons that the Scheme $S_7^{[1D]}$ is the best among the chosen schemes followed by S_4^{1D}. These comparisons can be quantified by introducing Resolving efficiency.

2.3. Resolving Efficiency

The resolving efficiency [7] of any numerical scheme,

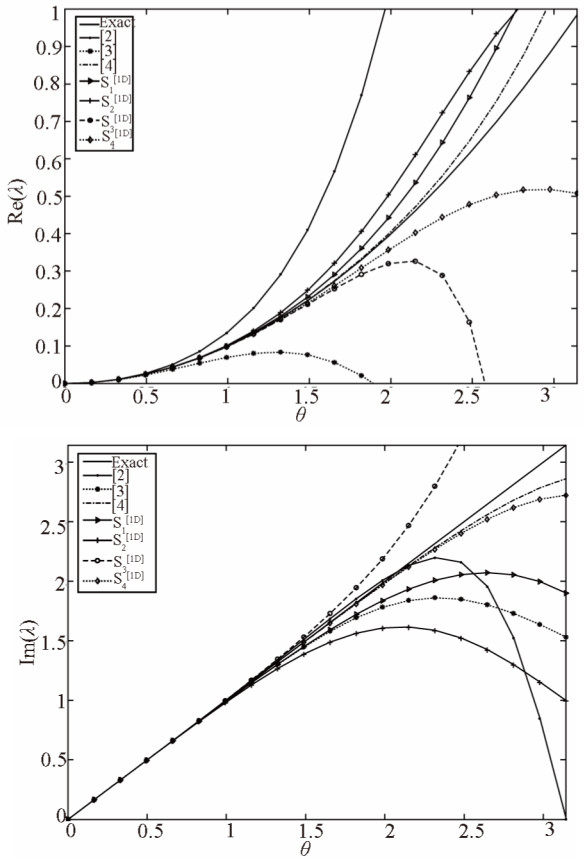

Figure 2. Comparison of real and imaginary parts of $\lambda^{[1D]}$ at $p = 10$.

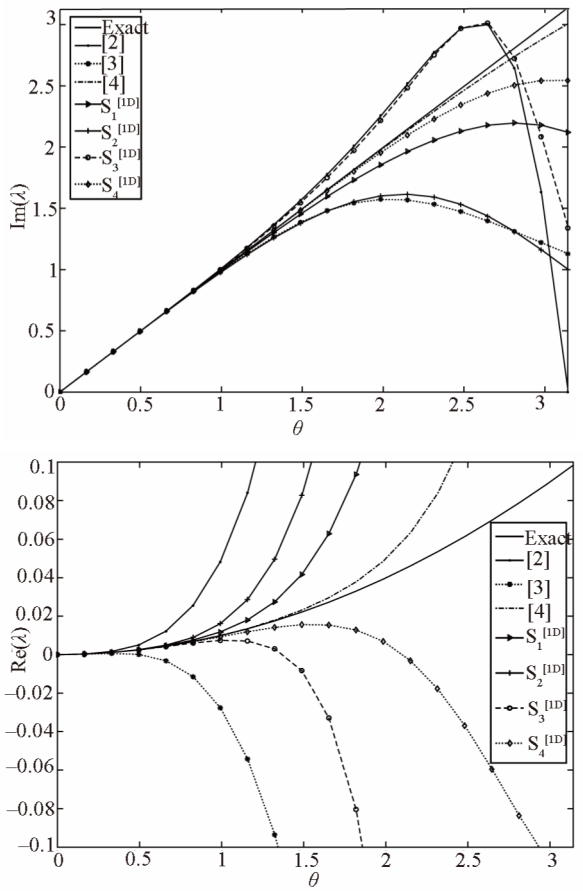

Figure 3. Comparison of real and imaginary parts of $\lambda^{[1D]}$ at $p = 100$.

defined by $\frac{\varphi_{max}}{\pi}$, is a number between 0 and 1. φ_{max}, independent of the grid size, is the maximum value of φ for which $|\lambda_{fd} - \lambda_{exact}|$ is less than a tolerance δ. Resolving efficiencies are computed for various schemes with different tolerance limits δ and presented in **Tables 1**, **2** and **3**, for peclet numbers 0.1, 10 and 100, respectively. It is clear from these tables that Scheme in [4] has a very good resolving efficiency followed by $S_4^{[1D]}$. Also, a careful look at these tables reveals that, for small peclet numbers, say for $p = 0.1$, all the fourth order schemes have more or less equal resolving efficiency, however, for $p = 10$ and 100, the fourth order schemes with four parameters have a much better resolving efficiency than the Schemes given in [2] and [3]. Since $Re(\lambda)$ of these schemes resolved to a much less value for $p = 10$ and 100, these are more prone to dissipation error which ultimately results into loss of accuracy. To demonstrate the effect of the resolution of various schemes on the accuracy of the generated numerical solutions, these schemes have been used to solve few model problems and compared their error norms in the next subsection.

2.4. Verification with Numerical Examples

Two distinct one-dimensional problems with sharp boundary layers are chosen for the purpose of numerical verification.

2.4.1. Example

Consider $-\varepsilon u_{xx} + u_x = \varepsilon\pi^2 \sin \pi x + \pi \cos \pi x$, $0 < \varepsilon << 1$, $0 < x < 1$ for which $u(x) = \sin \pi x + (e^{x/\varepsilon} - 1)/(e^{1/\varepsilon} - 1)$ is the exact solution with a sharp boundary layer, for small values of ε, towards $x = 1$.

2.4.2. Example

Consider $-\varepsilon u_{xx} + u_x = \frac{\varepsilon}{(1+x\,\varepsilon)^2} + \varepsilon\left(\frac{\varepsilon^2}{(1+x\,\varepsilon)^2} + \pi^2 \cos \pi x\right) - \pi \sin \pi x$, $0 < \varepsilon << 1$, $0 < x < 1$ for which $u(x) = \ln(1 + x\varepsilon) + \cos \pi x$ is the exact solution.

Table 1. Resolving efficiency of the real and imaginary parts of $\lambda^{[1D]}$ at $p = 0.1$.

	Re($\lambda^{[1D]}$)			Im($\lambda^{[1D]}$)		
Scheme	$\delta = 0.1$	$\delta = 0.01$	$\delta = 0.001$	$\delta = 0.1$	$\delta = 0.01$	$\delta = 0.001$
$S_1^{[1D]}$	0.68	0.39	0.22	0.65	0.38	0.22
$S_2^{[1D]}$	0.55	0.30	0.17	0.53	0.30	0.17
$S_3^{[1D]}$	0.70	0.42	0.24	0.68	0.42	0.24
$S_4^{[1D]}$	1.00	0.75	0.52	0.83	0.60	0.42
Scheme [2]	0.69	0.38	0.21	0.52	0.29	0.16
Scheme [3]	0.70	0.42	0.24	0.55	0.32	0.18
Scheme [4]	0.95	0.67	0.45	0.89	0.64	0.44

Table 2. Resolving efficiency of the real and imaginary parts of $\lambda^{[1D]}$ at $p = 10$.

	Re($\lambda^{[1D]}$)			Im($\lambda^{[1D]}$)		
Scheme	$\delta = 0.1$	$\delta = 0.01$	$\delta = 0.001$	$\delta = 0.1$	$\delta = 0.01$	$\delta = 0.001$
$S_1^{[1D]}$	0.59	0.32	0.18	0.68	0.37	0.21
$S_2^{[1D]}$	0.44	0.24	0.13	0.52	0.28	0.16
$S_3^{[1D]}$	0.56	0.33	0.19	0.63	0.37	0.22
$S_4^{[1D]}$	0.64	0.36	0.20	0.95	0.66	0.45
Scheme [2]	0.16	0.05	0.01	0.77	0.39	0.20
Scheme [3]	0.18	0.05	0.01	0.63	0.42	0.24
Scheme [4]	0.87	0.59	0.45	1.00	0.69	0.46

Table 3. Resolving efficiency of the real and imaginary parts of $\lambda^{[1D]}$ at $p = 100$.

	Re($\lambda^{[1D]}$)			Im($\lambda^{[1D]}$)		
Scheme	$\delta = 0.1$	$\delta = 0.01$	$\delta = 0.001$	$\delta = 0.1$	$\delta = 0.01$	$\delta = 0.001$
$S_1^{[1D]}$	0.31	0.16	0.11	0.74	0.42	0.21
$S_2^{[1D]}$	0.21	0.16	0.11	0.53	0.32	0.16
$S_3^{[1D]}$	0.26	0.16	0.11	0.63	0.37	0.21
$S_4^{[1D]}$	0.36	0.21	0.16	0.89	0.63	0.42
Scheme [2]	0.05	0.05	0.05	0.58	0.32	0.21
Scheme [3]	0.05	0.05	0.05	0.52	0.32	0.21
Scheme [4]	0.57	0.42	0.26	1.00	0.73	0.52

Model problems (2.4.1.) and (2.4.2.) are solved using the seven schemes $S_1^{[1D]}$ and $S_7^{[1D]}$. To vary the peclet number, the number of nodes has been varied from 11 to 81 and the diffusion parameter has been varied between 10^{-1} and 10^{-4}. The errors, computed using the infinity norm, are compared in the **Tables 4** and **5** for problems (2.4.1.) and (2.4.2.), respectively (read 1.234567(–08) as 1.234567×10^{-08} in all these tables).

The comparison of the error norms for various schemes reveals that for the peclet number p less than one, the accuracy of all the fourth order schemes are more or less equal however, the accuracy of the solutions of the S_1^{1D} to S_3^{1D} becomes better over schemes in [2] and [3] if p is increased to 1. The improvement in the accuracy becomes even better, better by two decimal places, if p is increased to 10 or more. This behavior supports the characteristic analysis carried out in the earlier section wherein we have shown that the resolving efficiency of schemes in [2] and [3] is much smaller than the other fourth order schemes at large peclet numbers. This concludes that to develop fourth order schemes using four parameters may improve the resolving efficiency and hence the accuracy of the numerical schemes. The same is also can be concluded between the sixth order schemes. The solutions generated using Scheme in [4] are uniformly far superior, for the entire range of peclet numbers 0.1 to 100, over all the schemes, where as S_4^{1D} is comparable only at low peclet numbers. Further, between the three developed fourth order schemes, S_2^{1D} has less resolving efficiency and the solutions obtained using this scheme are slightly inferior when compared with the other two, however, it is still has a better performance than the two existing three parameter schemes.

3. 2D Convection-Diffusion Equations

Efficiency of every numerical scheme can be established computationally by solving a class of example problems but analysis of the used numerical scheme is more important to gain confidence before applying them for real world problems. Usually, the efficiency of the higher order compact schemes for one-dimensional stationary CDE is shown by studying their monotonicity or comparing their characteristic curves. For 2D schemes, the comparisons have to be made characteristic surfaces. The development of a 2D scheme for the two-dimensional CDE (1) is already presented in [4] and using a similar procedure, 2D equivalents for the schemes S_1^{1D} to S_4^{1D} can be developed as follows:

3.1. ECHO Schemes

The development of an ECHO scheme for a two dimensional CDE will be given in a general procedure such that a similar procedure can be followed for different source functions. When the convection coefficients are constant, the two-dimensional equivalent of (4) is given by

$$-\alpha_h D_h^2 u_{i,j} - \alpha_k D_k^2 u_{i,j} + cD_h u_{i,j} + dD_k u_{i,j} = F^*_{i,j} \quad (17)$$

where $D_h u_{ij} = (u_{i+1,j} - u_{i-1,j})/2h$, $D_h^2 u_{ij} = (u_{i+1,j} - 2u_{ij}$

Table 4. Comparison of the error norms for the example 2.4.1.

ε	N	p	Scheme [4]	Scheme [3]	Scheme [2]	$S_4^{[1D]}$	$S_3^{[1D]}$	$S_2^{[1D]}$	$S_1^{[1D]}$
	11	1	9.09604(−08)	2.49708(−04)	3.72418(−04)	5.82331(−07)	2.77555(−05)	1.08028(−04)	4.03898(−05)
10^{-1}	21	1/2	1.43583(−09)	1.77531(−05)	2.33358(−05)	9.10599(−09)	1.70241(−06)	6.76222(−06)	2.53384(−06)
	41	1/4	2.24904(−11)	9.74330(−07)	1.46099(−06)	1.42770(−10)	1.05873(−07)	4.22750(−07)	1.58500(−07)
	81	1/8	3.51524(−13)	6.09526(−08)	9.14209(−08)	2.22867(−12)	6.60876(−09)	2.64234(−08)	9.90844(−09)
	11	10	8.88729(−08)	1.77531(−03)	2.29850(−03)	3.65241(−06)	4.88874(−05)	1.37564(−04)	4.53176(−05)
10^{-2}	21	5	1.44506(−09)	1.62385(−04)	2.29640(−04)	8.90909(−08)	2.43375(−06)	7.90343(−06)	2.75463(−06)
	41	2.5	2.25920(−11)	1.22054(−05)	1.79906(−05)	1.72607(−09)	1.22122(−07)	4.48986(−07)	1.63784(−07)
	81	1.25	3.52121(−13)	8.11830(−07)	1.21217(−06)	2.89799(−11)	6.89257(−09)	2.68860(−08)	1.00024(−08)
	11	100	8.77791(−08)	2.45467(−03)	2.54243(−03)	4.19056(−06)	6.92138(−05)	1.61527(−04)	4.75106(−05)
10^{-3}	21	50	1.48553(−09)	2.97753(−04)	3.20284(−04)	1.31316(−07)	4.37339(−06)	1.06444(−05)	3.17153(−06)
	41	25	2.40075(−11)	3.46001(−05)	3.96217(−05)	4.02580(−09)	2.56511(−07)	6.58354(−07)	2.01890(−07)
	81	12.5	3.77197(−13)	3.75653(−06)	4.71988(−06)	1.17706(−10)	1.37725(−08)	3.83374(−08)	1.23077(−08)
	11	1000	8.74623(−08)	2.54393(−03)	2.54569(−03)	4.20028(−06)	7.21326(−05)	1.64144(−04)	4.74090(−05)
10^{-4}	21	500	1.48149(−09)	3.19490(−04)	3.21770(−04)	1.32418(−07)	4.75839(−06)	1.10378(−05)	3.17837(−06)
	41	250	2.40094(−11)	3.97058(−05)	4.03276(−05)	4.14605(−09)	3.02745(−07)	7.10714(−07)	2.05097(−07)
	81	125	3.81699(−13)	4.88803(−06)	5.04161(−06)	1.29496(−10)	1.88050(−08)	4.47559(−08)	1.30083(−08)

Table 5. Comparison of the error norm for the example 2.4.2.

ε	N	p	Scheme [4]	Scheme [3]	Scheme [2]	$S_4^{[1D]}$	$S_3^{[1D]}$	$S_2^{[1D]}$	$S_1^{[1D]}$
	11	1	1.43890(−07)	1.94626(−04)	2.89270(−04)	4.22688(−07)	4.32687(−05)	1.70161(−04)	6.35454(−05)
10^{-1}	21	1/2	2.23695(−09)	1.24756(−05)	1.86690(−05)	6.76779(−09)	2.63582(−06)	1.04996(−05)	3.93304(−06)
	41	1/4	3.49160(−11)	7.83288(−07)	1.17424(−06)	1.06559(−10)	1.64206(−07)	6.56127(−07)	2.45980(−07)
	81	1/8	5.45044(−13)	4.90114(−08)	7.35061(−08)	1.67111(−11)	1.02436(−08)	4.09636(−08)	1.53605(−08)
	11	10	1.96384(−07)	8.40121(−04)	1.06619(−03)	1.67762(−06)	1.04588(−04)	3.00805(−04)	9.83965(−05)
10^{-2}	21	5	2.97619(−09)	8.06763(−05)	1.13353(−04)	4.36902(−08)	4.94140(−06)	1.62042(−05)	5.63472(−06)
	41	2.5	4.51730(−11)	6.21577(−06)	9.14492(−06)	8.72299(−10)	2.42789(−07)	8.96202(−07)	3.26724(−07)
	81	1.25	6.98417(−13)	4.16436(−07)	6.21489(−07)	1.47730(−11)	1.36489(−08)	5.33073(−08)	1.98291(−08)
	11	100	2.00935(−07)	1.12598(−03)	1.13629(−03)	1.85818(−06)	1.52895(−04)	3.65401(−04)	1.06674(−04)
10^{-3}	21	50	3.16771(−09)	1.42618(−04)	1.51699(−04)	6.19806(−08)	9.18371(−06)	2.25840(−05)	6.70649(−06)
	41	25	4.94835(−11)	1.69497(−05)	1.93126(−05)	1.95897(−09)	5.25029(−07)	1.35391(−06)	4.14529(−07)
	81	12.5	7.64628(−13)	1.86159(−06)	2.33386(−06)	5.81487(−11)	2.78268(−08)	7.76336(−08)	2.49046(−08)
	11	1000	2.00962(−07)	1.16355(−03)	1.13359(−03)	1.85569(−06)	1.59831(−04)	3.72624(−04)	1.06834(−04)
10^{-4}	21	500	3.16938(−09)	1.52631(−04)	1.51914(−04)	6.23029(−08)	1.00195(−05)	2.34902(−05)	6.74224(−06)
	41	250	4.96365(−11)	1.94022(−05)	1.95976(−05)	2.01159(−09)	6.21278(−07)	1.46575(−06)	4.22341(−07)
	81	125	7.76046(−13)	2.41622(−06)	2.48556(−06)	6.37930(−11)	3.80936(−08)	9.08791(−08)	2.63944(−08)

$+u_{i-1,j})/h^2$ and $D_k u_{ij} = (u_{i,j+1} - u_{i,j-1})/2k$, $D_k^2 u_{ij} = (u_{i,j+1} - 2u_{ij} + u_{i,j-1})/k^2$ over a uniformly distributed nodal points with step lengths h and k along $x-$ and $y-$ directions, respectively and discrete source function F_{ij} is a 2D equivalent of the corresponding 1D scheme. The development of the 2D ECHO scheme is

given bellow for different selection of source functions.

3.1.1. Scheme $S_1^{[1D]}$

Consider the source function, which is an extension of the scheme 2.1.1., given by

$$\begin{aligned} F^*_{ij} &= c_1 f_{i-1,j} + c_2 f_{ij} + c_3 f_{i+1,j} + c_4 (f_x)_i \\ &+ d_1 f_{i,j-1} + d_2 f_{ij} + d_3 f_{i,j+1} + d_4 (f_y)_{ij} \end{aligned} \tag{18}$$

The truncation error of the scheme (17) with the source function (18) computed using Taylor series expansion, is given by,

$$\begin{aligned} TE &= E u_{xyi,j} + G u_{xyyi,j} + H u_{xxyi,j} \\ &+ K u_{xxyyi,j} + f_{i,j} + O(h^4) \end{aligned} \tag{19}$$

where $E = dK_1 + cL_1$, $G = -bK_1 + cL_2$, $H = dK_2 - aL_1$, $K = -bK_2 - aL_2$

$$\begin{aligned} K_1 &= h(c_3 - c_1) + c_4,\ K_2 = h^2 (c_3 + c_1)/2, \\ L_1 &= k(d_3 - d_1) + d_4,\ L_2 = k^2 (d_3 + d_1)/2 \end{aligned} \tag{20}$$

Expanding the terms in (19) and (20) shows that the scheme (17) is of second order accurate. To make it fourth order, the scheme and the source function is written as

$$\begin{aligned} &\left(-\alpha_h D_h{}^2 - \alpha_k D_k{}^2 + cD_h + dD_k + ED_h D_k \right. \\ &\left. + GD_k{}^2 D_h + HD_h{}^2 D_k + KD_h{}^2 D_k{}^2 \right) u_{ij} = F_{ij} \\ &F_{i,j} = c_1 f_{i-1,j} + c_2 f_{i,j} + c_3 f_{i+1,j} + c_4 f_{xi,j} \\ &\quad + d_1 f_{i,j-1} + d_2 f_{i,j} + d_3 f_{i,j+1} + d_4 f_{yi,j} \end{aligned} \tag{21}$$

where the coefficients c_i and d_i, $i = 1, 2, 3 \& 4$ are given by

$$c_1 = \frac{1}{6} - 3\beta_x{}^3 + \beta_x{}^2 - 0.5\beta_x + 3\beta_x{}^2 \gamma_x - \beta_x \gamma_x + 0.25\gamma_x,$$

$$c_2 = \frac{2}{3} - 2\beta_x{}^2 + 2\beta_x \gamma_x,$$

$$c_3 = \frac{1}{6} + 3\beta_x{}^3 + \beta_x{}^2 + 0.5\beta_x - 3\beta_x{}^2 \gamma_x - \beta_x \gamma_x - 0.25\gamma_x,$$

$$d_1 = \frac{1}{6} - 3\beta_y{}^3 + \beta_y{}^2 - 0.5\beta_y + 3\beta_y{}^2 \gamma_y - \beta_y \gamma_y + 0.25\gamma_y,$$

$$d_2 = \frac{2}{3} - 2\beta_y{}^2 + 2\beta_y \gamma_y,$$

$$d_3 = \frac{1}{6} + 3\beta_y{}^3 + \beta_y{}^2 + 0.5\beta_y - 3\beta_y{}^2 \gamma_y - \beta_y \gamma_y - 0.25\gamma_y,$$

$$d_4 = h(-6\beta_y{}^3 - 0.5\gamma_y + 6\beta_y{}^2 \gamma_y),$$

$$\beta_x = \frac{a}{ch},\ \beta_y = \frac{a}{dk},\ \gamma_x = \frac{\alpha_h}{ch}, \text{ and } \gamma_y = \frac{\alpha_k}{dk}$$

for c and d not equal to zero

and $c_1 = \frac{1}{12}$, $c_2 = \frac{5}{6}$, $c_3 = \frac{1}{12}$, $c_4 = 0$, $d_1 = \frac{1}{12}$, $d_2 = \frac{5}{6}$, $d_3 = \frac{1}{12}$, $d_4 = 0$ when $c = d = 0$.

Similarly, for the other selection of source functions remainder terms are utilized to get fourth order accuracy. For every scheme E, G, H and K are same as in (20) but K_1, K_2, L_1 and L_2 varies with the scheme.

3.1.2. Scheme $S_2^{[1D]}$

$$\begin{aligned} F_i &= f_i + c_1 (f_x)_{i-1,j} + c_2 (f_x)_{ij} + c_3 (f_x)_{i+1,j} \\ &+ d_1 (f_y)_{i,j-1} + d_2 (f_y)_{ij} + d_3 (f_y)_{i,j+1} \\ \text{Let} \quad & K_1 = c_1 + c_2 + c_3,\ K_2 = h(c_3 - c_1), \\ & L_1 = d_1 + d_2 + d_3,\ L_2 = k(d_3 - d_1) \end{aligned} \tag{22}$$

The coefficients in the discrete source function are given by

$$c_1 = h\left(\begin{array}{l} \frac{1}{6}\beta_x + \beta_x{}^3 - 0.5\beta_x{}^2 - \frac{1}{12} \\ -\frac{1}{12}\gamma_x - \beta_x{}^2 \gamma_x + 0.5\beta_x \gamma_x \end{array}\right),$$

$$c_2 = h\left(\frac{2}{3}\beta_x - 2\beta_x{}^3 - \frac{5}{6}\gamma_x + 2\beta_x{}^2 \gamma_x\right),$$

$$c_3 = h\left(\begin{array}{l} \frac{1}{6}\beta_x + \beta_x{}^3 + 0.5\beta_x{}^2 + \frac{1}{12} \\ -\frac{1}{12}\gamma_x - \beta_x{}^2 \gamma_x - 0.5\beta_x \gamma_x \end{array}\right),$$

$$d_1 = k\left(\begin{array}{l} \frac{1}{6}\beta_y + \beta_y{}^3 - 0.5\beta_y{}^2 - \frac{1}{12} \\ -\frac{1}{12}\gamma_y - \beta_y{}^2 \gamma_y + 0.5\beta_y \gamma_y \end{array}\right),$$

$$d_2 = k\left(\frac{2}{3}\beta_y - 2\beta_y{}^3 - \frac{5}{6}\gamma_y + 2\beta_y{}^2 \gamma_y\right),$$

$$d_3 = k\left(\begin{array}{l} \frac{1}{6}\beta_y + \beta_y{}^3 + 0.5\beta_y{}^2 + \frac{1}{12} \\ -\frac{1}{12}\gamma_y - \beta_y{}^2 \gamma_y - 0.5\beta_y \gamma_y \end{array}\right)$$

for $c = d \neq 0$ and $c_1 = \frac{-h}{24}$, $c_2 = 0$, $c_3 = \frac{h}{24}$, $d_1 = \frac{-k}{24}$, $d_2 = 0$, $d_3 = \frac{k}{24}$ when $c = d = 0$.

3.1.3. Scheme $S_3^{[1D]}$

$$\begin{aligned} F_{ij} &= f_{ij} + c_1 (f_x)_{ij} + c_2 (f_{xx})_{ij} + c_3 (f_{xxx})_{ij} \\ &+ d_1 (f_y)_{ij} + d_2 (f_{yy})_{ij} + d_3 (f_{yyy})_{ij} \\ \text{Let} \quad & K_1 = c_1,\ K_2 = c_2,\ L_1 = d_1,\ L_2 = d_2, \end{aligned} \tag{23}$$

The coefficients in the discrete source function are given by

$$c_1 = h(\beta_x - \gamma_x),\ c_2 = h^2\left(\frac{1}{6} + \beta_x^2 - \beta_x\gamma_x\right),$$
$$c_3 = h^3\left(\beta_x^3 + \frac{1}{6}\beta_x - \beta_x^2\gamma_x - \frac{1}{12}\gamma_x\right),\ d_1 = k(\beta_y - \gamma_y),$$
$$d_2 = k^2\left(\frac{1}{6} + \beta_y^2 - \beta_y\gamma_y\right),$$
$$d_3 = k^3\left(\beta_y^3 + \frac{1}{6}\beta_y - \beta_y^2\gamma_y - \frac{1}{12}\gamma_y\right)$$

for c and d not equal to zero and $c_1 = 0$, $c_2 = \frac{h^2}{12}$, $c_3 = 0$, $d_1 = 0$, $d_2 = \frac{k^2}{12}$, $d_3 = 0$ when $c = d = 0$.

3.1.4. Scheme $S_4^{[1D]}$

$$F_i = c_1 f_{i-1,j} + c_2 f_{ij} + c_3 f_{i+1,j} + c_4 (f_x)_i + c_5 (f_{xx})_i + d_1 f_{i-1,j} + d_2 f_{ij} + d_3 f_{i+1,j} + d_4 (f_y)_i + d_5 (f_{yy})_i - f_{ij} \quad (24)$$

Let

$$K_1 = c_4 + h(c_3 - c_1),\ K_2 = c_5 + \frac{h^2}{2}(c_3 + c_1),$$
$$L_1 = d_4 + k(d_3 - d_1),\ L_2 = d_5 + \frac{k^2}{2}(d_3 + d_1),$$

The coefficients in the discrete source function are given by

$$c_1 = 12\beta_x^4 - 3\beta_x^3(1 + 4\gamma_x) + \beta_x^2(2 + 3\gamma_x) - \beta_x(0.5 + \gamma_x) + (0.1 + 0.25\gamma_x),$$
$$c_2 = -24\beta_x^4 + 24\beta_x^3\gamma_x - 4\beta_x^2 + 2\beta_x\gamma_x + 0.8,$$
$$c_3 = 12\beta_x^4 + 3\beta_x^3(1 - 4\gamma_x) + \beta_x^2(2 - 3\gamma_x) + \beta_x(0.5 - \gamma_x) + (0.1 - 0.25\gamma_x),$$
$$c_4 = -h(6\beta_x^3 - 6\beta_x^2\gamma_x + 0.5\gamma_x),$$
$$c_5 = -h^2\left(12\beta_x^4 - 12\beta_x^3\gamma_x + \beta_x^2 - \frac{1}{15}\right),$$
$$d_1 = 12\beta_y^4 - 3\beta_y^3(1 + 4\gamma_y) + \beta_y^2(2 + 3\gamma_y) - \beta_y(0.5 + \gamma_y) + (0.1 + 0.25\gamma_y),$$
$$d_2 = -24\beta_y^4 + 24\beta_y^3\gamma_y - 4\beta_y^2 + 2\beta_y\gamma_y + 0.8,$$
$$d_3 = 12\beta_y^4 + 3\beta_y^3(1 - 4\gamma_y) + \beta_y^2(2 - 3\gamma_y) + \beta_y(0.5 - \gamma_y) + (0.1 - 0.25\gamma_y),$$
$$d_4 = -k(6\beta_y^3 - 6\beta_y^2\gamma_y + 0.5\gamma_y),$$
$$d_5 = -k^2\left(12\beta_y^4 - 12\beta_y^3\gamma_y + \beta_y^2 - \frac{1}{15}\right)$$

for c and d not equal to zero and $c_1 = \frac{1}{30}$, $c_2 = \frac{14}{15}$, $c_3 = \frac{1}{30}$, $c_4 = 0$, $c_5 = \frac{h^2}{20}$, $d_1 = \frac{1}{30}$, $d_2 = \frac{14}{15}$, $d_3 = \frac{1}{30}$, $d_4 = 0$, $d_5 = \frac{k^2}{20}$ when $c = d = 0$.

These four different schemes 3.1.1.-3.1.4. are compared with the existing ECHO schemes given in [2] and [3].

2D Scheme in [2] :

$$F_i = c_1 f_{i-1,j} + c_2 f_{ij} + c_3 f_{i+1,j} + d_1 f_{i-1,j} + d_2 f_{ij} + d_3 f_{i+1,j} - f_{ij}$$

Let

$$K_1 = h(c_3 - c_1),\ K_2 = \frac{h^2}{2}(c_3 + c_1), \quad (25)$$
$$L_1 = k(d_3 - d_1),\ L_2 = \frac{k^2}{2}(d_3 + d_1),$$

The coefficients in the discrete source function are given by

$$c_1 = \frac{1}{6} + (\beta_x - \gamma_x)(\beta_x - 0.5),\ c_2 = \frac{2}{3} - 2\beta_x(\beta_x - \gamma_x),$$
$$c_3 = \frac{1}{6} + (\beta_x - \gamma_x)(\beta_x + 0.5),$$
$$d_1 = \frac{1}{6} + (\beta_y - \gamma_y)(\beta_y - 0.5),\ d_2 = \frac{2}{3} - 2\beta_y(\beta_y - \gamma_y),$$
$$d_3 = \frac{1}{6} + (\beta_x - \gamma_x)(\beta_x + 0.5)$$

for c and d not equal to zero and $c_1 = \frac{1}{12}$, $c_2 = \frac{5}{6}$, $c_3 = \frac{1}{12}$, $d_1 = \frac{1}{12}$, $d_2 = \frac{5}{6}$, $d_3 = \frac{1}{12}$ when $c = d = 0$.

2D Scheme in [3] :

$$F_i = f_{i,j} + c_1 (f_x)_{ij} + c_2 (f_{xx})_{i,j} + d_1 (f_y)_{ij} + d_2 (f_{yy}) f_{ij} \quad (26)$$

Let

$$K_1 = c_1,\ K_2 = c_2,\ L_1 = d_1,\ L_2 = d_2,$$

The coefficients in the discrete source function are given by

$$c_1 = h(\beta_x - \gamma_x),\ c_2 = h^2(0.5 + \beta_x(\beta_x - \gamma_x)),$$
$$d_1 = h(\beta_x - \gamma_x),\ d_2 = h^2(0.5 + \beta_x(\beta_x - \gamma_x))$$

for c and d not equal to zero and $c_1 = 0$, $c_2 = \frac{h^2}{12}$,

$$d_1 = 0\,,\ \ d_2 = \frac{h^2}{12} \quad \text{when} \quad c = d = 0\,.$$

3.2. Comparison of the Characteristic Surfaces

The characteristic surface of a differential equation is obtained in terms of peclet numbers $p_x = \frac{ch}{a}$ and $p_y = \frac{dk}{a}$, in $x-$ and $y-$ directions, respectively. The characteristic of the governing Equation (1), obtained by substituting $e^{I(w_x x + w_y y)}$ in the place of the dependent variable u, is given by:

$$\lambda^{[2D]} = \frac{cd}{a}\frac{1}{p_x p_y}\left(\left(r\theta_x^2 + \frac{\theta_y^2}{r}\right) + I\left(p_x r\theta_x + \frac{p_y\theta_y}{r}\right)\right) \quad (27)$$

where $\theta_x = w_x h$, $\theta_x = w_y k$ are phase angles and w_x, w_y are the wave numbers, h and k are step lengths and $I = \sqrt{-1}$. Similarly, the characteristic surface of any difference scheme is also obtained by substituting $e^{I(i\theta_x + j\theta_y)}$ for u_{ij} in the difference scheme. Following this procedure, the characteristic surfaces of the 2D schemes $S_1^{[2D]}$ to $S_4^{[2D]}$ are computed and the same are given by

Characteristic Surface for $S_1^{[1D]}$:

$$\lambda_1^{2D} = \frac{cd}{a}\frac{1}{p_x p_y}\left(\frac{z_1 + Iz_2}{z_3 + Iz_4}\right) \quad (28)$$

$$z_1 = 2r\gamma_h(1-\cos\theta_x) + \frac{2\gamma_k}{r}(1-\cos\theta_y)$$
$$-\left(\frac{p_y}{p_x r}(1-\gamma_h) + \frac{p_x r}{p_y}(1-\gamma_h)\right)\sin\theta_x \cdot \sin\theta_y \quad ;$$
$$-\frac{1}{r}\left(\frac{1-\gamma_h}{rp_x^2} + r\frac{1-\gamma_k}{p_y^2} + \frac{r}{6} + \frac{1}{r6}\right)(2\cos\theta_x - 2)(2\cos\theta_y - 2)$$

$$z_2 = p_x r\sin\theta_x + \frac{p_y}{r}\sin\theta_y +$$
$$\left(\frac{r}{p_y}(1-\gamma_k) + \frac{p_x r}{6} - \frac{1-\gamma_h}{p_x r}\right)\sin\theta_x(2\cos\theta_y - 2) + \quad ;$$
$$\left(\frac{p_y}{rp_x^2}(1-\gamma_h) + \frac{p_y}{6r} - \frac{r}{p_y}(1-\gamma_k)\right)(2\cos\theta_x - 2)\sin\theta_y$$

$$z_3 = (\mu_2 + \xi_2 - 1) + (\mu_3 + \mu_1)\cos\theta_x + (\xi_3 + \xi_1)\cos\theta_y\,,$$
$$z_4 = (\mu_3 - \mu_1)\sin\theta_x + (\xi_3 - \xi_1)\sin\theta_y + \mu_4\theta_x + \xi_4\theta_y$$

where

$$\gamma_h = \frac{p_x}{2}\coth\frac{p_x}{2}\,,\ \ \gamma_k = \frac{p_y}{2}\coth\frac{p_y}{2}\,,$$

$$\mu_1 = \frac{1}{6} - \frac{3(1-\gamma_h)}{p_x^3} + \frac{1-\gamma_h}{p_x^2} - \frac{2-\gamma_h}{4p_x}\,,\ \ \mu_2 = \frac{2}{3} - \frac{2(1-\gamma_h)}{p_x^2}\,,$$
$$\mu_3 = \frac{1}{6} + \frac{3(1-\gamma_h)}{p_x^3} + \frac{1-\gamma_h}{p_x^2} + \frac{2-\gamma_h}{4p_x}\,,$$
$$\mu_4 = -\frac{6(1-\gamma_h)}{p_x^3} - \frac{\gamma_h}{2p_x}\,.$$

Similarly,

$$\xi_1 = \frac{1}{6} - \frac{3(1-\gamma_k)}{p_y^3} + \frac{1-\gamma_k}{p_y^2} - \frac{2-\gamma_k}{4p_y}\,,\ \ \xi_2 = \frac{2}{3} - \frac{2(1-\gamma_k)}{p_y^2}\,,$$
$$\xi_3 = \frac{1}{6} + \frac{3(1-\gamma_k)}{p_y^3} + \frac{1-\gamma_k}{p_y^2} + \frac{2-\gamma_k}{4p_y}\,,$$
$$\xi_4 = -\frac{6(1-\gamma_k)}{p_y^3} - \frac{\gamma_k}{2p_y}\,.$$

The terms z_3 and z_4 in the denominator of (28) are the contributions due to the source function of the scheme and hence vary from scheme to scheme. However, the numerator of all the exponential schemes are same as in (28). To justify this, one can expand K_1, K_2, L_1 and L_2 with their parameters for every scheme and in each case they appear like

$$K_1 = \frac{a-\alpha_h}{c}\,,\ \ K_2 = \frac{h^2}{6} + \frac{a(a-\alpha_h)}{c^2}\,,$$
$$L_1 = \frac{b-\alpha_k}{d}\,,\ \ L_2 = \frac{k^2}{6} + \frac{b(b-\alpha_k)}{d^2}\,.$$

Therefore, the characteristics of the schemes are differ by their denominator which contains the contribution of the source function of the scheme. The characteristic surfaces of the remaining three schemes are

Characteristic Surface for $S_2^{[1D]}$:

$$\lambda_2^{[2D]} = \frac{cd}{a}\frac{1}{p_x p_y}\left(\frac{z_1 + Iz_2}{z_3 + Iz_4}\right) \quad (29)$$

$$z_3 = 1 - (\mu_3 - \mu_1)\theta_x\sin\theta_x - (\xi_3 - \xi_1)\theta_y\cos\theta_y\,,$$
$$z_4 = \mu_2\theta_x + \xi_2\theta_y + (\mu_3 + \mu_1)\theta_x\cos\theta_x + (\xi_3 + \xi_1)\theta_y\cos\theta_y\,,$$
$$\mu_1 = \frac{1-\gamma_h}{p_x^3} - \frac{1-\gamma_h}{2p_x^2} + \frac{2-\gamma_h}{12p_x} - \frac{1}{12}\,,$$
$$\mu_2 = \frac{2}{3p_x} - \frac{5\gamma_h}{6p_x} - \frac{2(1-\gamma_h)}{p_x^3}\,,$$
$$\mu_3 = \frac{1-\gamma_h}{p_x^3} + \frac{1-\gamma_h}{2p_x^2} + \frac{2-\gamma_h}{12p_x} + \frac{1}{12}\,,$$
$$\xi_1 = \frac{1-\gamma_k}{p_y^3} - \frac{1-\gamma_k}{2p_y^2} + \frac{2-\gamma_k}{12p_y} - \frac{1}{12}\,,$$
$$\xi_2 = \frac{2}{3p_y} - \frac{5\gamma_k}{6p_y} - \frac{2(1-\gamma_k)}{p_y^3}\,,$$

$$\xi_3 = \frac{1-\gamma_k}{p_y^3} + \frac{1-\gamma_k}{2p_y^2} + \frac{2-\gamma_k}{12p_y} + \frac{1}{12};$$

Characteristic Surface for $S_3^{[1D]}$:

$$\lambda_3^{2D} = \frac{cd}{a}\frac{1}{p_x p_y}\left(\frac{z_1 + Iz_2}{z_3 + Iz_4}\right) \tag{30}$$

$$z_3 = 1-\mu_2\theta_x^2 - \xi_2\theta_y^2,\ z_4 = \mu_1\theta_x + \xi_1\theta_y - \mu_3\theta_x^3 - \xi_3\theta_y^3,$$

$$\mu_1 = \frac{1-\gamma_h}{p_x},\ \mu_2 = \frac{1}{6} + \frac{1-\gamma_h}{p_x^2},\ \mu_3 = \frac{1-\gamma_h}{p_x^3} + \frac{2-\gamma_h}{12p_x},$$

$$\xi_1 = \frac{1-\gamma_k}{p_y},\ \xi_2 = \frac{1}{6} + \frac{1-\gamma_k}{p_y^2},\ \xi_3 = \frac{1-\gamma_k}{p_y^3} + \frac{2-\gamma_k}{12p_y},$$

Characteristic Surface for $S_4^{[1D]}$:

$$\lambda_4^{2D} = \frac{cd}{a}\frac{1}{p_x p_y}\left(\frac{z_1 + Iz_2}{z_3 + Iz_4}\right) \tag{31}$$

$$z_3 = (\mu_2 + \xi_2 - 1) + (\mu_3 + \mu_1)\cos\theta_x + (\xi_3 + \xi_1)\cos\theta_y - \mu_5\theta_x^2 - \xi_5\theta_y^2,$$

$$z_4 = (\mu_3 - \mu_1)\sin\theta_x + (\xi_3 - \xi_1)\sin\theta_y + \mu_4\theta_x + \xi_4\theta_y,$$

$$\mu_1 = \frac{12(1-\gamma_h)}{p_x^4} - \frac{3(1-\gamma_h)}{p_x^3} + \frac{2-\gamma_h}{p_x^2} - \frac{2-\gamma_h}{4p_x} + \frac{1}{10},$$

$$\mu_2 = \frac{4}{5} - \frac{24(1-\gamma_h)}{p_x^3} - \frac{2(2-\gamma_h)}{p_x^2},$$

$$\mu_3 = \frac{12(1-\gamma_h)}{p_x^4} + \frac{3(1-\gamma_h)}{p_x^3} + \frac{2-\gamma_h}{p_x^2} + \frac{2-\gamma_h}{4p_x} + \frac{1}{10},$$

$$\mu_4 = -\frac{6(1-\gamma_h)}{p_x^3} - \frac{\gamma_h}{2p_x},\ \mu_5 = -\frac{12(1-\gamma_h)}{p_x^4} - \frac{1}{p_x^2} + \frac{1}{15};$$

$$\xi_1 = \frac{12(1-\gamma_k)}{p_y^4} - \frac{3(1-\gamma_k)}{p_y^3} + \frac{2-\gamma_k}{p_y^2} - \frac{2-\gamma_k}{4p_y} + \frac{1}{10},$$

$$\xi_2 = \frac{4}{5} - \frac{24(1-\gamma_k)}{p_y^3} - \frac{2(2-\gamma_k)}{p_y^2},$$

$$\xi_3 = \frac{12(1-\gamma_k)}{p_y^4} + \frac{3(1-\gamma_k)}{p_y^3} + \frac{2-\gamma_k}{p_y^2} + \frac{2-\gamma_k}{4p_y} + \frac{1}{10},$$

$$\xi_4 = -\frac{6(1-\gamma_k)}{p_y^3} - \frac{\gamma_k}{2p_y}, \xi_5 = -\frac{12(1-\gamma_k)}{p_y^4} - \frac{1}{p_y^2} + \frac{1}{15};$$

Similarly, the characteristics of the schemes in [2] and [3] are derived and given by

Characteristic Surface for Scheme [2]:

$$\lambda^{[2]} = \frac{cd}{a}\frac{1}{p_x p_y}\left(\frac{z_1 + iz_2}{z_3 + iz_4}\right) \tag{32}$$

$$z_3 = (\mu_2 + \xi_2 - 1) + (\mu_3 + \mu_1)\cos\theta_x + (\xi_3 + \xi_1)\cos\theta_y,$$

$$z_4 = (\mu_3 - \mu_1)\sin\theta_x + (\xi_3 - \xi_1)\sin\theta_y,$$

$$\mu_1 = \frac{1-\gamma_h}{p_x},\quad \mu_2 = \frac{1}{6} + \frac{1-\gamma_h}{p_x^2},$$

$$\xi_1 = \frac{1-\gamma_k}{p_y},\quad \xi_2 = \frac{1}{6} + \frac{1-\gamma_k}{p_y^2}.$$

Characteristic Surface for Scheme [3]:

$$\lambda^{[3]} = \frac{cd}{a}\frac{1}{p_x p_y}\left(\frac{z_1 + iz_2}{z_3 + iz_4}\right) \tag{33}$$

$$z_3 = 1-\mu_2\theta_x^2 - \xi_2\theta_y^2, z_4 = \mu_1\theta_x + \xi_1\theta_y,$$

$$\mu_1 = \frac{1-\gamma_h}{p_x},\quad \mu_2 = \frac{1}{6} + \frac{1-\gamma_h}{p_x^2},$$

$$\xi_1 = \frac{1-\gamma_k}{p_y},\quad \xi_2 = \frac{1}{6} + \frac{1-\gamma_k}{p_y^2}.$$

The characteristic surfaces defined in (28-31) are symmetric or antisymmetric in the region $[0, -\pi]\times[0, -\pi]$ depending on whether $\lambda_i^{[2D]}$ is an even or odd function of p_x and p_y. Further they are also periodic with period 2π. These surfaces $\lambda_i^{[2D]}$, with respect to $0 \le p_x \le \pi$ and $0 \le p_y \le \pi$, can be plotted together for the shake of comparison, however, unlike in one dimensional case, it is difficult to visualize the closeness of these surfaces. Alternatively, comparisons are made at different angular cross sections from the origin. Further, if $p_x = p_y$, they are also symmetric with respect to 45˚ curve, therefore, in the present case, the values of the characteristics are compared at 15˚, 30˚ and 45˚ cross sections.

The characteristics at the three chosen cross sections are plotted against the exact one in **Figures 4** and **5** for $p_x = p_y = 10$ and $p_x = p_y = 100$, respectively. The comparisons of the real parts of the characteristics are included in the first column of these figures, while the comparisons of the imaginary parts are shown in the second column. The three rows in these figures stand for the comparisons at 15˚, 30˚ and 45˚ cross sections, respectively.

It can be seen clearly in each of these figures that the characteristics of the existing three parameter 2D schemes are far away from the exact curve compared to the four parameter schemes which have been developed in this work. Interestingly, the deviation is increased with angle and also with peclet number giving a very substantial deviation at $p_x = p_y = 100$. Particularly, Scheme in [2] is deviated more at the center and also produced a significant overshoot for all most all the cross sections.

Among the present four parameter based fourth order 2D schemes, $S_2^{[2D]}$ produced minimum and $S_3^{[2D]}$ produced maximum dissipation errors. However, when

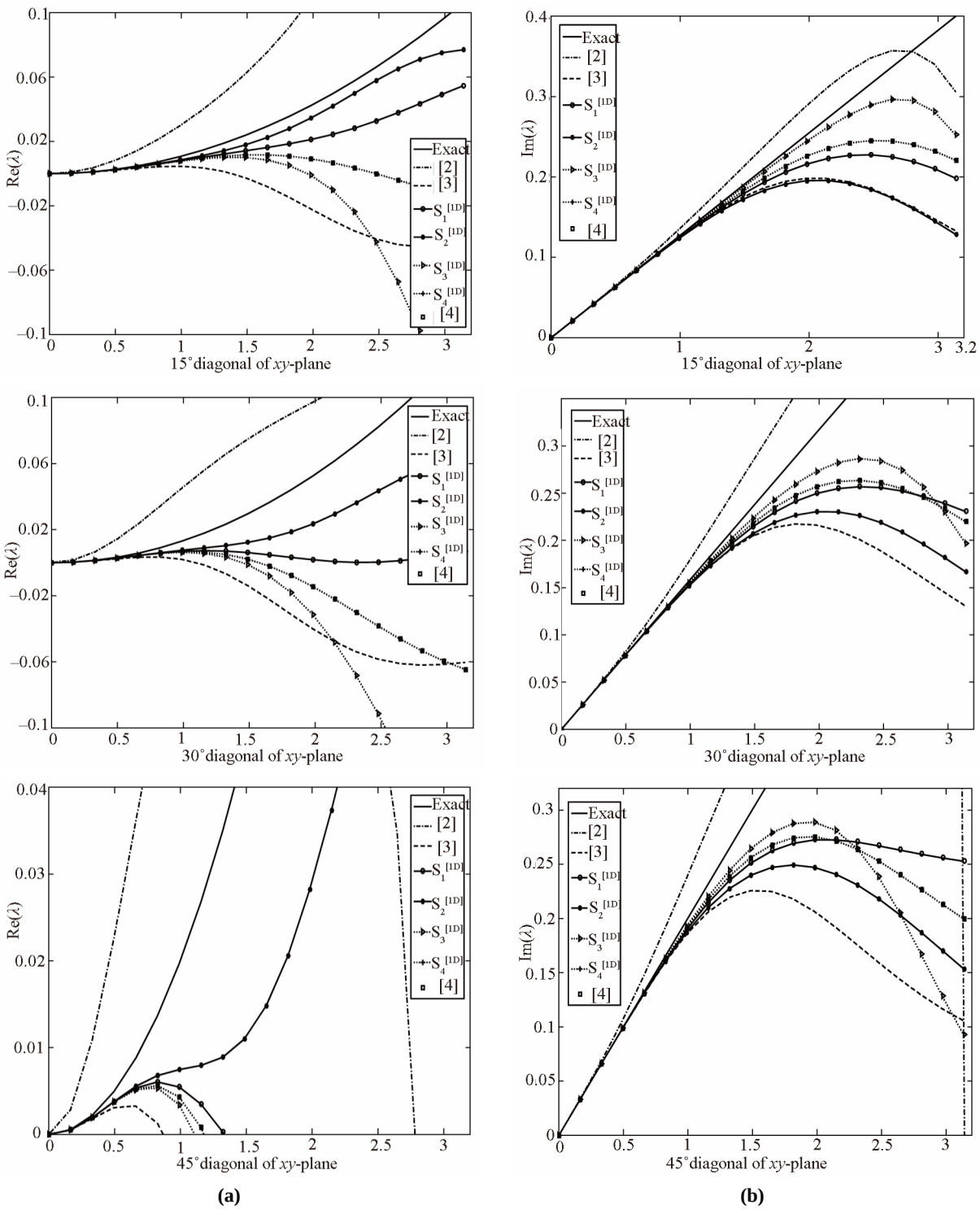

Figure 4. Comparison of the (a) real and (b) imaginary parts of the characteristic at $p_x = p_y = 10$.

the peclet number is increased to 100, $S_2^{[2D]}$ overshot the exact characteristic in its real part but there is no such abnormality with respect to $S_3^{[2D]}$. A similar overshoot in its real part is also been observed in $S_1^{[2D]}$ at least along 15° cross section. For the imaginary parts, $S_3^{[2D]}$ has the minimum and $S_2^{[2D]}$ has the high deviation

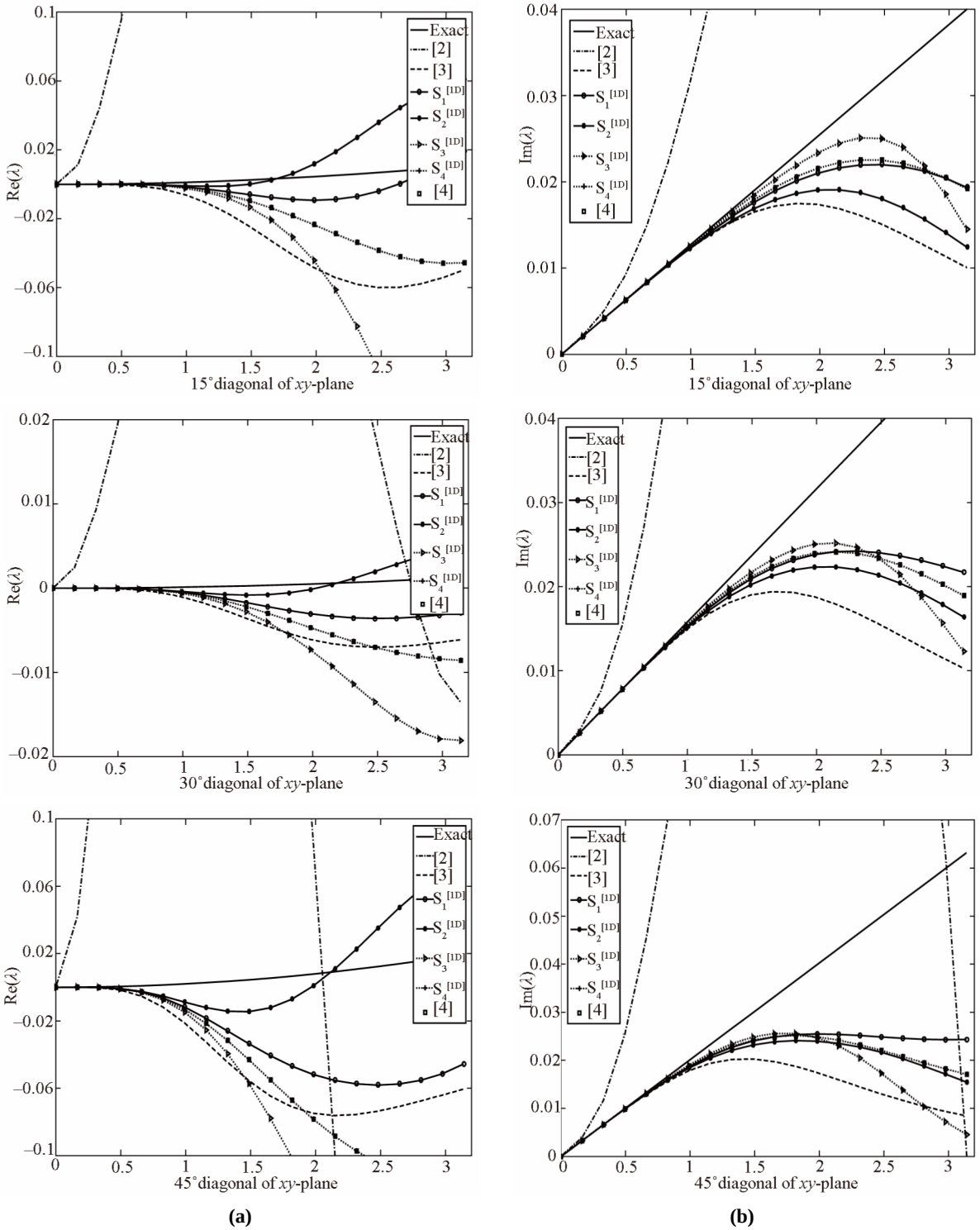

Figure 5. Comparison of the (a) real and (b) imaginary parts of the characteristic at $p_x = p_y = 100$.

giving little more dispersion error. To conclude, $S_3^{[2D]}$ may be relative a better one among the developed four parameter schemes. However, both five and six parameter based schemes are indistinguishable and these are better resolved for real case as comparable to $S_3^{[2D]}$ and almost close to $S_3^{[2D]}$ for imaginary case.

Table 6. Comparison of the error norm and rate of convergence for the example 3.3.1.

ε	N	(p_x, p_y)	Scheme [4]	Rate	$S_4^{[2D]}$	Rate	$S_3^{[2D]}$	Rate	$S_2^{[2D]}$	Rate	$S_1^{[2D]}$	Rate
	11×11	(2, 1)	3.2758(−05)		3.3534(−05)		1.0116(−04)		2.4911(−04)		7.5792(−05)	
10^{-1}	21×21	(1, 1/2)	2.1086(−06)	3.98	2.1208(−06)	3.98	6.4702(−06)	4.0	1.5813(−05)	3.98	4.6762(−06)	4.20
	41×41	(1/2, 1/4)	1.3299(−07)	3.99	1.3317(−07)	3.99	4.0445(−07)	4.0	9.8422(−07)	4.01	2.9358(−07)	3.99
	81×81	(1/4, 1/2)	8.3358(−09)	4.00	8.3364(−09)	3.99	2.5290(−08)	4.0	6.1618(−08)	4.00	1.8314(−08)	4.00
	11×11	(20, 10)	1.0280(−01)		8.2609(−02)		6.3122(−02)		8.4654(−01)		1.7722(−01)	
10^{-2}	21×21	(10, 5)	5.9942(−03)	4.10	9.3313(−03)	2.48	2.7119(−02)	1.22	1.3763(−01)	2.62	4.2111(−02)	2.07
	41×41	(5, 5/2)	1.7187(−04)	5.12	3.5268(−04)	4.73	3.3219(−03)	3.03	1.3880(−02)	3.31	4.9041(−03)	3.10
	81×81	(5/2, 5/4)	2.9582(−06)	5.86	6.5424(−06)	5.75	2.2380(−04)	3.89	9.0323(−04)	3.94	3.3340(−04)	3.88
	11×11	(200,100)	2.9329(01)		1.2625(−00)		2.0891(−04)		1.0339(02)		2.1052(−00)	
10^{-3}	21×21	(100,50)	6.7439(00)	2.12	6.2716(−01)	1.00	2.8535(−05)	2.87	2.5296(01)	2.03	1.0482(−00)	1.00
	41×41	(50,25)	1.3939(00)	2.27	3.0705(−01)	1.03	2.3053(−03)	−6.34	6.0623(00)	2.06	5.1798(−01)	1.02
	81×81	(25, 25/2)	2.1120(−01)	2.72	1.2556(−01)	1.29	5.2316(−02)	−4.50	1.3821(00)	2.13	2.3966(−01)	1.11
	161×161	(25/2,25/4)	1.6135(−02)	3.71	2.0981(−02)	2.58	4.1933(−02)	0.32	2.5399(−01)	2.44	7.1006(−02)	1.76
	321×321	(25/4,25/8)	5.7798(−04)	4.80	1.0951(−03)	4.26	6.9254(−03)	2.60	2.9998(−02)	3.08	1.0272(−02)	2.79

3.3. Numerical Verification

Consider the following two-dimensional problems with sharp boundary layers.

3.3.1. Example

$$-\varepsilon u_{xx} - \varepsilon u_{yy} + 2u_x + u_y =$$
$$2^{-\frac{1}{\varepsilon}}\left(\frac{1}{\varepsilon}+1\right)y(1+y)^{\left(\frac{1}{\varepsilon}-1\right)} - e^{y-x}(1+2\varepsilon),\quad 0<\varepsilon<<1,$$

in the region $0 \le x,\ y \le 1$ with exact solution

$$u(x,y) = e^{y-x} + 2^{-\frac{1}{\varepsilon}}(1+y)^{1+\frac{1}{\varepsilon}}.$$

3.3.2. Example

$$\varepsilon u_{xx} + \varepsilon u_{yy} + u_x + u_y = (1-2y)\exp\left(\frac{-x}{\varepsilon}\right),\quad 0<\varepsilon<<1,$$

in the region $0 \le x,\ y \le 1$ with exact solution

$$u(x,y) = \left(y(1-y) - 2\varepsilon x\right)\exp\left(\frac{-x}{\varepsilon}\right).$$

The example problems (3.3.1.) and (3.3.2.) are solved using $S_1^{[2D]}$ to $S_4^{[2D]}$ and also with the scheme given in [4]. The results are compared, in the form of error norm and the rate of convergence, in **Tables 6** and **7**, for problems (3.3.1.) and (3.3.2.), respectively. As expected, the scheme given in [4] and the scheme $S_4^{[2D]}$ produced higher rate of convergence for Example 3.3.1. and better accuracy for Example 3.3.2.. These comparisons are once again confirm the accuracy of the characteristic analysis made in the previous subsection.

For convection dominated problems all most all the schemes produced same accuracy however, it has been shown in [4] that the scheme given in [4] has performed better than the schemes given [2] and [3]. Looking at the characteristic analysis and numerical verification, it can be concluded that it is better to use n parameter based 2D schemes to develop n^{th} order schemes, over schemes with less parameters.

Table 7. Comparison of the error norm and rate of convergence for the example 3.3.2.

ε	N	(p_x, p_y)	Scheme [4]	Rate	$S_4^{[2D]}$	Rate	$S_3^{[2D]}$	Rate	$S_2^{[2D]}$	Rate	$S_1^{[2D]}$	Rate
	11×11	(1,1)	2.2658(–04)		2.2675(–04)		1.8741(–04)		3.9867(–04)		2.9060(–04)	
10^{-1}	21×21	(1/2, 1/2)	1.4046(–05)	4.00	1.4048(–05)	4.00	1.1519(–05)	4.02	2.4501(–05)	4.02	1.7917(–05)	4.02
	41×41	(1/4, 1/4)	8.7539(–07)	4.00	8.7542(–07)	4.00	7.1382(–07)	4.01	1.5323(–06)	4.00	1.1212(–06)	4.00
	81×81	(1/8, 1/8)	5.5187(–08)	3.99	5.5187(–08)	3.99	4.4908(–08)	3.99	9.6631(–08)	3.99	7.0682(–08)	3.99
	11×11	(10,10)	9.6530(–03)		1.2891(–02)		1.4054(–02)		3.6026(–02)		1.6494(–02)	
10^{-2}	21×21	(5,5)	4.6367(–03)	1.06	4.9883(–03)	1.37	5.0340(–03)	1.48	1.1336(–02)	1.67	6.8089(–03)	1.28
	41×41	(5/2, 5/2)	9.4892(–04)	2.29	9.5928(–04)	2.38	8.1280(–04)	2.63	2.0086(–03)	2.50	1.3281(–03)	2.36
	81×81	(5/4, 5/4)	9.0223(–05)	3.39	9.0385(–05)	3.40	6.9922(–05)	3.54	1.8443(–04)	3.45	1.2511(–04)	3.41
	11×11	(100,100)	5.7441(–02)		1.8322(–02)		1.9735(–02)		2.7883(–01)		2.2093(–02)	
10^{-3}	21×21	(50,50)	1.0511(–02)	2.45	1.0879(–02)	0.75	1.1782(–02)	0.74	8.8185(–02)	–1.66	1.3292(–02)	0.73
	41×41	(25,25)	6.6370(–04)	3.99	5.8353(–03)	0.90	6.3558(–03)	0.89	2.7366(–02)	1.69	7.2365(–03)	0.88
	81×81	(25/2, 25/2)	1.6570(–03)	–1.32	2.6765(–03)	1.12	2.9415(–03)	1.11	8.1345(–03)	1.75	3.4111(–03)	1.08
	161×161	(25/4, 25/4)	8.5246(–04)	0.99	9.6240(–04)	1.48	1.0164(–03)	1.53	2.2469(–03)	1.86	1.2841(–03)	1.41
	321×321	(25/8, 25/8)	2.0814(–04)	2.03	2.1228(–04)	2.18	1.8988(–04)	2.42	4.4575(–04)	2.33	2.9124(–04)	2.14

4. Conclusions

In this work we have developed and made characteristics based comparisons for exponential compact schemes. The characteristic comparisons are also been extended for two dimensional problems. It can be concluded from this short analysis that when exponential compact higher order schemes are generated by evaluating the source term as a linear combination of its values at the surrounding nodal points and its derivatives, it is better to use n parameters to generate an n^{th} order scheme so that the resultant scheme will have a better resolution and hence can produce more accurate solutions. For the same reason, the fourth order ECHO schemes developed in this work are more accurate than the existing schemes [2,3]. The same is also true when the ECHO schemes are extended for 2D CDE, the corresponding three parameter schemes are comparatively less efficient than the four or six parameter based schemes.

5. Acknowledgements

Author Nachiketa Mishra is greatly indebted to the Council of Scientific and Industrial Research for the financial support 09/084(0389)/2006-EMR-I.

6. References

[1] E. C. Gartland, Jr., "Uniform High-Order Difference Schemes for a Singularly Perturbed Two-Point Boundary Value Problem," *Mathematics of Computation*, Vol. 48, No. 178, 1987, pp. 551-564. doi:10.1090/S0025-5718-1987-0878690-0

[2] A. C. R. Pillai, "Fourth-Order Exponential Finite Difference Methods for Boundary Value Problems of Convective Diffusion Type," *International Journal for Numerical Methods in Fluids*, Vol. 37, No. 1, 2001, pp. 87-106. doi:10.1002/fld.167

[3] Z. F. Tian and S. Q. Dai, "High-Order Compact Exponential Finite Difference Methods for Convection-Di-

ffusion Type Problems," *Journal of Computational Physics*, Vol. 220, No. 2, 2007, pp. 952-974. doi:10.1016/j.jcp.2006.06.001

[4] Y. V. S. S. Sanyasiraju and N. Mishra, "Spectral Resolutioned Exponential Compact Higher Order Scheme (SRECHOS) for Convection-Diffusion Equation," *Computer Methods in Applied Mechanics and Engineering*, Vol. 197, No. 51-52, 2008, pp. 4737-4744. doi:10.1016/j.cma.2008.06.013

[5] A. M. Il'in, "A Difference Scheme for a Differential Equation with a Small Parameter Multiplying the Highest Derivative (Russian)," *Matematicheskie Zametki*, Vol. 6, No. 2, 1969, pp. 237-248.

[6] D. You, "A High-Order Padé ADI Method for Unsteady Convection-Diffusion Equations," *Journal of Computational Physics*, Vol. 214, No. 1, 2006, pp. 1-11. doi:10.1016/j.jcp.2005.10.001

[7] S. K. Lele, "Compact Finite Difference Schemes with Spectral-Like Resolution," *Journal of Computational Physics*, Vol. 103, No. 1, 1992, pp. 16-42. doi:10.1016/0021-9991(92)90324-R

